HHS Public Access

Author manuscript

*Oncogene*. Author manuscript; available in PMC 2017 January 27.

Published in final edited form as:

*Oncogene*. 2017 January 26; 36(4): 512–524. doi:10.1038/onc.2016.222.

# *cel-mir-237* and its homologue, hsa-miR-125b, modulate the cellular response to ionizing radiation

**Chanatip Metheetrairut**[1,4,*], **Brian D. Adams**[1,2,*], **Sunitha Nallur**[3], **Joanne B. Weidhaas**[3,5], and **Frank J. Slack**[1,2,6]

[1]Department of Molecular, Cellular and Developmental Biology, Yale University, New Haven, CT 06520, USA

[2]Institute for RNA Medicine, Department of Pathology, BIDMC Cancer Center/Harvard Medical School, Boston, MA 02215, USA

[3]Department of Therapeutic Radiology, Yale University School of Medicine, New Haven, CT 06520 USA

## Abstract

Elucidating the mechanisms involved in sensitizing radioresistant tumors to ionizing radiation (IR) treatments while minimizing injury to surrounding normal tissue is an important clinical goal. Due to their sequence-derived specificity and properties as gene regulators in IR-affected pathways, microRNAs (miRNAs) could serve as adjuvant therapeutic agents that alter cellular sensitivity to radiation treatment. To identify radiosensitizing miRNAs, we initially utilized the *C. elegans* vulval cell model, an *in vivo* system developed to study IR-dependent radiosensitivity as a measure of clonogenic cell death. We tested several candidate miRNA deletion mutants post γ-irradiation and identified *cel-mir-237* as a miRNA which when deleted caused animals to be more resistant to IR, while *cel-mir-237* overexpressing strains were IR-sensitive. Additionally, wild-type animals downregulated *cel-mir-237* levels post IR in a time-dependent manner. We identified *jun-1* (JUN transcription factor homolog) as a novel target of *cel-mir-237*. Specifically, *jun-1* transcript levels increased in wild-type animals post-γ-irradiation, and loss of *cel-mir-237* also resulted in higher *jun-1* expression. As expected, loss of *jun-1* resulted in IR sensitivity, similar to the phenotype of *cel-mir-237* overexpressors. Since miR-237 is the homologue of human miR-125, we validated our findings in MCF-7 and MDA-MB-231 breast cancer cell lines, which harbor lower hsa-miR-125b levels than normal HMECs. Forced expression of hsa-miR-125b in these cells resulted in radiosensitivity, as seen by reduced clonogenic survival, enhanced apoptotic activity, and enhanced senescence post IR. Finally, re-expression of c-JUN in MDA-MB-231 cells promoted radio-resistance and abrogated miR-125-mediated radio-sensitization. Our findings



[6]Corresponding Author: Frank Slack, Ph.D. Department of Pathology, BIDMC Cancer Center/Harvard Medical School, 3 Blackfan Circle, Boston MA 02115, Telephone: 617-735-2601; Fax: (617) 735-2646; fslack@bidmc.harvard.edu.
[4]Current address: Department of Biochemistry, Faculty of Medicine Siriraj Hospital, Mahidol University, Bangkok, 10700, Thailand
[5]Current addres: Division of Molecular and Cellular Oncology, UCLA School of Medicine, Los Angeles, CA 90095, USA
[*]These authors contributed equally to this work

**Disclosure of Conflicts of Interest:** Authors have no conflicts of interest to disclose

Supplementary Information accompanies the paper on the Oncogene website (http://www.nature.com/onc)

suggest that overexpression of *cel-mir-237* and its homologue, hsa-miR-125b, functions as sensitizers to γ-irradiation in both a nematode *in vivo* model and breast cancer cells, and could potentially be utilized as an adjuvant therapeutic to enhance radiation sensitivity.

**Keywords**

microRNAs; Breast Cancer; Radiation Therapy; miR-125b; *C. elegans*

## Introduction

Ionizing radiation (IR) affects cells by generating DNA double-strand breaks (DSB) resulting in a cellular response involving a complex network of pathways that includes DNA replication, DNA-repair, and programmed cell death[1]. These DSBs are repaired through homologous recombination (HR) or non-homologous end-joining (NHEJ) DNA-repair mechanisms[2,3]. This process of normal DNA-repair is disrupted in cancer cells, and is one of the reasons why cytotoxic radiation-based therapeutic approaches are still a primary treatment modality for many cancer patients. Unfortunately, despite a number of advancements in the field of radiobiology, a significant number of patients suffer from locoregional recurrence due to the outgrowth of radioresistant cells[4]. Dose-escalation approaches to eradicating residual tumor cells are met with significant acute and chronic toxicities that arise from the effects of radiotherapy on surrounding normal tissue, limiting the use and subsequent effectiveness of this treatment. Therefore it is essential to develop novel strategies to sensitize cancer cells to radiation-based therapies.

MicroRNAs (miRNAs) are small non-coding RNAs that regulate gene expression post-transcriptionally, either through mRNA degradation or translational inhibition[5–7]. MiRNAs regulate gene expression by base pairing with complementary sequences in the 3′ untranslated region (3′ UTR) of protein-coding transcripts, and function as master regulators of gene expression[7,8]. Dysregulation of a particular miRNA family can promote disease states such as cancer by modulating cellular pathways that control differentiation, apoptosis, and survival[9–12]. Restoration of these cancer-associated miRNAs either by inhibition (i.e., antagomiRs) or re-introduction (i.e., miRNA mimics) strategies has been shown to reduce tumorigenic properties such as cell growth and invasion, while promoting apoptosis and sensitivity to chemotherapeutic agents[13–17]. Importantly, miRNAs have previously been shown to be critical in the cellular response to radiation[18], and to act as modifiers of the radiation response both *in vivo* in a *Caenorhabditis elegans* model of radiosensitivity, and in cancer cells[19–21].

In this study, we utilized a *C. elegans* model of radiosensitivity to assay for radiation-induced reproductive cell death[22]. Tissue multipotent precursor cells have an ability to self-renew and divide to generate invariant cell lineages in a manner analogous to the cancer stem cell system[23–25], and this model has been shown to represent non-apoptotic, clonogenic cell death, analogous to the most common form of cell death in tumors. Therefore, use of this model to further confirm the genetic components of radiosensitivity of these cells is a useful step toward altering radio-therapeutic outcome.

We sought to identify miRNAs that could function as sensitizers to γ-irradiation, which we envision could be used as a neoadjuvant during IR treatment. We tested several candidate miRNA deletion mutant nematodes after γ-irradiation for a radiosensitive phenotype, and identified *cel-mir-237* as a miRNA able to alter radiation sensitivity. Upon further investigation the *cel-miR-237* homologue, hsa-miR-125b, was also found to promote γ-irradiation sensitivity in MCF-7 and MDA-MB-231 breast cancer cell lines. Both *cel-miR-237* and hsa-miR-125b induce this radiation-sensitivity in part by targeting and downregulating *JUN*. Importantly, altering c-JUN expression in either *C. elegans* or breast cancer cells lines resulted in altered sensitivity to radiation treatments. This data suggests that miR-125b could be used as a potential adjuvant to radiation therapies to enhance radiosensitivity.

## Results

### cel-mir-237(tm2238) deletion results in radioresistance in C. elegans cells after γ-irradiation

We previously identified miRNAs with altered expression in response to γ-irradiation[20]. To confirm which of these responsive miRNAs could function as radio-sensitizers *in vivo*, we identified the *C. elegans* homologues of these miRNAs(Table 1). We then performed experiments where various *C. elegans* strains harboring loss-of-function mutations in these miRNA genes (herein termed deletion mutants) were irradiated and scored for radiosensitivity based on the presence of previously defined γ-irradiation-dependent morphological vulval defects[22]. In this model, vulval defects are the metric of radiosensitivity, and represent reproductive cell death. While a majority of the deletion mutant strains tested resulted in no change or in sensitization to γ-irradiation(Fig. S1A & Table 1), only the *mir-237(tm2238)* deletion mutant displayed a significant radioresistant phenotype(Fig. 1A). Furthermore, *cel-mir-237* levels significantly decreased in wild-type N2 animals 6-9hrs post IR, and remained low at later time points(Fig. 1B). This is in contrast to other miRNAs tested, where the respective levels change ~16-24hrs post γ-irradiation(Fig. S1B). The only other miRNA whose levels decreased post-IR(Fig. 1B) and whose loss of function promotes an IR-resistant phenotype in *C. elegans* is *let-7*[20]. This finding suggests that loss of *cel-mir-237* predicts radioresistance.

### cel-mir-237 overexpression sensitizes C. elegans to γ-irradiation

To confirm that *cel-mir-237* was important in the γ-irradiation-response, we tested whether overexpression of *cel-mir-237* protected *C. elegans* from γ-irradiation. Two integrated *unc-119(ed3);[Cbr unc-119::mir-237] cel-mir-237* overexpressing (o/e) strains were generated by bombardment and characterized(Fig. S1C). *cel-mir-237* copy number in o/e lines #7 and #44 were ~100- to 8-fold higher than N2 animals, respectively. This translated into ~80- to 20-fold higher expression of mature *cel-mir-237* than N2 animals, respectively. While no gross morphological defect was observed in these lines(Fig. 1D), upon γ-irradiation both *cel-mir-237* o/e lines displayed radiosensitivity(Fig. 1C & E). This confirms that miR-237 plays an important γ-irradiation-sensitizing role within a *C. elegans in vivo* model of radiosensitivity.

## cel-mir-237 functions through jun-1 in sensitizing cells to γ-irradiation

miRNAs function by fine-tuning gene expression through the control of particular genetic networks, therefore we sought to identify *cel-mir-237*-regulated γ-irradiation-response genes. We examined three targeting databases: miRanda[26,27], TargetScanWorm[28,29], and mirWIP[30], and identified 140 putative *cel-mir-237* mRNA targets(Fig. 2A, *left panel*). To reduce false positives, we examined putative targets predicted by more than one algorithm, and identified 30 *cel-mir-237* targets, 25 of which were conserved in humans(Table S1). We then generated an irradiation-response gene list that encompassed 216 genes, curated from sources including KEGG, Wormbook[31], and Haaften *et al.*[32], and involved processes such as DNA-damage response, cell survival, and cell proliferation(see Table S2 for details). When overlapping these two datasets, only *jun-1* was identified(Fig. 2A, *right panel*).

We then set out to verify whether *jun-1* and *cel-mir-237* operated within the same genetic pathway. *jun-1* is predicted to be a target of *mir-237*/*lin-4* family of miRNAs(Fig. S2A), and the *mir-237*-complemetary region within the *C. elegans jun-1* 3′ UTR is conserved in other nematode species(Fig. S2B). Furthermore, the murine miR-237 homologue, *mmu-miR-125b*, has been previously shown to directly target *Jun*[33], and *in situ* analyses by Feng *et al.* and Esquela-Kerscher *et al.* confirmed that both *jun-1*(Fig. S2C)[34] and *mir-237*[35] are expressed in a number of tissues including vulval muscle cells. We therefore examined *jun-1* levels in N2 animals in comparison to the *mir-237* deletion mutant and overexpressor strains. The levels of *jun-1* increased in animals with the *mir-237* locus deleted, while *jun-1* levels decreased in the *cel-mir-237* o/e strains, as compared to N2 animals(Fig. 2B). Furthermore, in N2 animals that had undergone γ-irradiation, the levels of *jun-1* significantly increased 9–24hrs post γ-irradiation(Fig. 2C). In the same samples, this expression profile was inversely correlated with *cel-mir-237*. Notably, *jun-1* levels became upregulated only at time-points after the observed changes in *cel-mir-237* levels, consistent with the notion of *jun-1* being controlled by *cel-mir-237*.

To test whether *jun-1* functioned as an integral part of the γ-irradiation response, *jun-1(gk551)* and *jun-1(gk557)* mutant strains were utilized to determine whether these loss-of-function lines would phenocopy the *cel-mir-237*-induced γ-irradiation phenotype, and show radiosensitivity. *jun-1* mutants do not have any obvious vulval defects prior to γ-irradiation. However, when subjected to increasing doses of γ-irradiation, both *jun-1* mutant lines were more radiosensitive than N2 animals(Fig. 2D). To assess whether *jun-1* and *cel-mir-237* operated within the same genetic pathway, epistatic experiments were performed. Here, *jun-1* mutants were each crossed with the radioresistant *mir-237(tm2238)* mutant strain. The resultant *mir-237*;*jun-1* double mutants still exhibited radiosensitivity(Fig. 2E). These results indicate that *jun-1* is both epistatic to and genetically downstream of *cel-mir-237*, and that loss of *jun-1* due to regulation by *cel-mir-237* sensitizes cells to DNA damaging agents such as γ-irradiation.

## The cel-mir-237 homologue, hsa-miR-125b, sensitizes breast cancer cells to γ-irradiation

Given the radiosensitizing role of *cel-mir-237* in our *in vivo* model of radiosensitivity, we investigated whether the homologous human miRNA, *hsa-miR-125*(Fig. 3A), could promote a similar phenotype in cancer cells. While it is unclear which miR-125 isoform is most

closely related to *cel-mir-237* we focused on hsa-miR-125b, since meta-data from miRBase indicated that it was expressed at higher levels than hsa-miR-125a. Furthermore, in METABRIC, the mean log2 expression of hsa-miR-125b-5p across all 1262 breast cancer samples was 13.38, as compared to 7.2, 8.59, or not detectable for hsa-miR-125a-3p, hsa-miR-125a-5p, or hsa-miR-125b-3p, respectively. Since proper development of *C. elegans* vulval precursor cells depend upon EGFR and NOTCH1 signaling, two aberrantly activated pathways in human breast cancer, we profiled both normal and breast cancer cell lines. In a vast majority of breast cancer lines miR-125b was downregulated compared to HMECs, MCF-10As, and a panel of conditionally reprogrammed normal breast cells (CRCs)[36](Fig. 3B & Fig. S3A), supporting the notion that miR-125b broadly functions as a tumor suppressor in breast cancer cell lines[37–39].

To investigate the role of miR-125b during γ-irradiation, HMECs, MCF-7, and MDA-MB-231 cell lines were profiled after treatment. Normal HMECs downregulated miR-125b levels as early as 4hrs post-IR, which rebounded by 16hrs post-IR(Fig. 3E & 3H). Interestingly, re-introduction of miR-125b alone promoted a pro-differentiation phenotype where cells became large, formed vacuolar structures, and had a heightened granular appearance(Fig. S3B). The persistent endogenous miR-125b levels observed post-IR coupled with the pro-differentiation phenotype could, in part, explain why ectopic expression of miR-125b did not sensitize these cells to γ-irradiation, but rather promoted a mild protective effect(Fig. S3C-E & 3J, *right panel*). Furthermore, addition of a miR-125b inhibitor did not protect HMECs from IR-induced cell death, as compared a control miRNA inhibitor(Fig. S3H). Overall, these findings suggest that while miR-125b itself functions by regulating cellular proliferation and differentiation pathways in normal mammary epithelial cells, it does not alter the sensitivity of these cells to DNA-damaging agents such as γ-irradiation.

Contrary to the effects in HMECs, breast cancer cell lines have variable responses to γ-irradiation. In MDA-MB-231 cells, miR-125b levels rapidly decreased in a dose-dependent manner and remained low after exposure to γ-irradiation(Fig. 3D & 3G), while in MCF-7 cells miR-125b levels fluctuated post γ-irradiation, which is most likely reflective of the low baseline levels of miR-125b(Fig. 3C & 3F). Importantly, in contrast to HMECs, both MCF-7 and MDA-MB-231 cell lines ectopically expressing miR-125b were sensitized to γ-irradiation(Fig. 3I), as compared to lines expressing a scrambled RNA control (miR-Scr). When MCF-7 cells were transfected with a miR-125b inhibitor γ-irradiation sensitivity was not altered(Fig. S3F), as expected given the low basal levels of miR-125b in these cells, while the miR-125b inhibitor promoted a mild protective effect in MDA-MB-231 cells(Fig. S3G).

### hsa-miR-125b promotes γ-irradiation induced senescence

To investigate the anti-growth phenotypes associated with miR-125b re-introduction post γ-irradiation, we functionally assessed breast cancer cell lines ectopically expressing miR-125b. We first tested cell proliferation by PI staining and found that while γ-irradiation promoted G2/M arrest[40,41], miR-125b did not significantly alter cell cycle distribution either alone or in combination with γ-irradiation(Fig. S4A). Instead, miR-125b transfected MDA-

MB-231 cells underwent striking morphological changes post-γ-irradiation indicative of senescence(Fig. 4A-B), and SA-β-gal assays performed on miR-125b transfected cells confirmed this senescence-promoting effect(Fig. 4C-D). We also observed significantly enhanced SA-β-gal levels in MCF-7 cells co-treated with miR-125b and 4-6-Gy γ-irradiation, as compared to miR-Scr and γ-irradiation treatments(Fig. 4E). These miR-125b-dependent effects were not observed in HMECs after γ-irradiation(Fig. S4C). Additionally, Annexin V staining assays indicated miR-125b transfected MDA-MB-231 cells were less likely to undergo γ-irradiation-induced apoptosis and DNA damage(Fig. S4B & S4D), further supporting the notion that miR-125b promotes a cytostatic phenotype when coupled with γ-irradiation. Together, these results suggest that while miR-125b alone does not induce cellular senescence, it does play an important role in priming breast cancer cells for subsequent radiation-induced senescence.

## Aberrant expression of c-JUN confers γ-irradiation sensitivity

Given mir-237/miR-125b modulation of *jun-1* was important in γ-irradiation sensitivity in *C. elegans*, we next asked whether the mammalian homologue of *jun-1*, *JUN*, was important during this process. We first screened for *JUN* levels in breast cancer lines, and found MCF-7 cells, which harbored the lowest miR-125b levels, had the highest levels of *JUN*(Fig. 5A). *JUN* levels also changed upon γ-irradiation treatment in breast cancer cells, concordant with the observed changes in miR-125b levels(Fig. 5B, *left and middle panels*). Given the low level of miR-125b in MCF-7 cells, the lack of an effect on *JUN* is not surprising. Though, MCF-7 cells at baseline are more sensitive to γ-irradiation as compared to MDA-MB-231 cells, which could in part be due to the low expression of c-JUN. The tendency for cancer cells to up-regulate *JUN* post γ-irradiation is in contrast to normal HMECs, where 16hrs after 2-4Gy treatment the levels of *JUN* were 2-fold lower than 0Gy treated cells(Fig. 5B, *right panel*), which inversely correlated with miR-125b levels. This further supports the notion that c-JUN is an important component of the γ-irradiation response.

To further assess the role of c-JUN, we generated c-JUN-ORF-IRES-GFP-MDA-MB-231 cell lines(Fig. S5A). We chose this line because it expressed low endogenous levels of *JUN*, and we observed a robust increase in *JUN* levels after γ-irradiation treatment, suggesting that c-JUN is important for cell survival during this process. This line expressed >14-fold more *JUN* transcript than an Empty-GFP-control line, and was not responsive to miR-125b mimic treatments(Fig. 5C). Endogenous *JUN* did not change in c-JUN-ORF-IRES-GFP versus parental lines, but decreased in abundance in the presence of miR-125b, as determined by a *JUN* 5′ UTR primer set, which is expected given miR-125b targets *JUN*[42]. Also as expected, c-JUN-ORF-IRES-GFP lines were more resistant to γ-irradiation as compared to GFP-control lines(Fig. 5D), and did not demonstrate sensitivity to miR-125b-induced γ-irradiation as compared to an Empty-GFP control line(Fig. 5E). We subsequently performed loss of function experiments in $JUN^{high}$ expressing MCF-7 cells, and found that two independent siRNAs to *JUN* could weakly sensitize these cells to γ-irradiation(Fig. 5F & S5B). Since there are multiple c-JUN family members that can generate an AP-1 transcription factor complex with c-FOS[43], MCF-7 cells were instead treated with Tanshinone IIA(Fig. S5C), an inhibitor of AP-1 DNA binding activity, which resulted in enhanced γ-irradiation sensitivity(Fig. S5D-E).

### hsa-miR-125b regulates MAPK signaling and activity of c-JUN

While investigating the role of the miR-125b-c-JUN regulatory axis during γ-irradiation-induced stress, we found that miR-125b inhibited the activity of c-JUN. Specifically, after 4Gy treatment, transfection with miR-125b mimic reduced c-JUN protein expression ~1.5- to 1.8-fold in MCF-7 and MDA-MB-231 cells, respectively(Fig. 6A-B). This is expected given previous reports of miR-125b targeting *JUN*[42]. However, these reductions were not observed in the absence of γ-irradiation(Fig. 6C-D). This indicated that miR-125b might also regulate a process that alters the activity and subsequently the stability of c-JUN. Indeed pSer73-c-JUN levels were downregulated 1.5- and 3.0-fold in miR-125b transfected MCF-7 and MDA-MB-231 cells, respectively(Fig. 6C-D), indicating the activity of upstream Jun N-terminal kinases (JNKs) was attenuated by miR-125b. To identify which signaling pathways were most affected by miR-125b, we performed qPCR array experiments on cells treated with γ-irradiation or miR-125b. We then overlapped genes that were 2-fold downregulated by miR-125b and 2-fold upregulated after γ-irradiation treatment, with all putative miR-125b targets as predicted by TargetScan(Fig. 6E). Using this analysis we identified several upstream kinases such as *MAP3K1* and *MAP2K7*, that were strongly elevated after γ-irradiation in both cell lines, yet were downregulated by miR-125b(Table S3). Interestingly, *MAP2K7* (JNK-activating kinase), *MAP3K1*, and *MEKK1*, have already been shown to be targets of miR-125b[44,45]. This analysis also identified several genes that were downregulated by miR-125b independent of γ-irradiation such as *MOS* and *HSPB1* in MCF-7 cells, *CDKN1A* and *SFN* in MDA-MB-231 cells, and *EGR1* in both cell lines. Given many of these genes are considered pro-tumorigenic, these findings support the notion that miR-125b has tumor-suppressive capabilities in breast cancer independent of promoting γ-irradiation sensitivity. While further studies are needed to determine which genes from our analysis are also targeted and regulated during miR-125b-induced γ-irradiation sensitivity, overall these data indicate that miR-125b can promote sensitivity to γ-irradiation by modulating the MAPK-c-JUN axis resulting in reduced expression of genes important for cell survival during DNA-damage induced cell stress(Fig. 6F).

## Discussion

Studying γ-irradiation response *in vivo* utilizing gene knockout models offers opportunities to determine how one genetic factor affects an entire organism after γ-irradiation-induced stress. Here we report the parallel roles of the two homologous miRNAs, *cel-mir-237* and hsa-miR-125b, in radiosensitization of a *C. elegans* model of clonogenic cell death and human breast cancer cells to γ-irradiation. In N2 nematodes, *cel-mir-237* was downregulated upon γ-irradiation, and functionally the loss of *cel-mir-237* protected cells from γ-irradiation, while overexpression of *cel-mir-237* promoted a radiosensitive phenotype. These results suggest that cells may actively downregulate *cel-mir-237* as a mechanism to promote survival during and after γ-irradiation. A similar mechanism may be in place in breast cancer cells, as we identified miR-125b to be downregulated after γ-irradiation treatment, and the forced expression of miR-125b to impart γ-irradiation sensitivity in MDA-MB-231 and MCF-7 cells, but not in normal HMEC cells. We also demonstrated that the JUN family proteins: *jun-1* in *C. elegans* and c-JUN in humans, were regulated by *cel-mir-237* and hsa-

miR-125b, respectively, and that altered expression of this family of proteins could modulate γ-irradiation sensitivity.

*cel-mir-237* is part of a miRNA family that includes *lin-4* and *mir-237*; is upregulated during the L2 to L3 transition in *C. elegans*[35,46,47], and may share certain functions with the heterochronic miRNA gene *lin-4*[48]. However, no phenotype has yet been reported for loss of this particular miRNA. Initially, we did not observe any gross morphologic or phenotypic defects in *cel-mir-237(tm2238)* deletion mutants maintained in an unstressed state, including those phenotypes tested by Miska *et al*[49]. However, once *cel-mir-237(tm2238)* deletion mutants were stressed with γ-irradiation, we observed striking vulval morphological defects due radiosensitivity and reproductive cell death. This is interesting, given most miRNA-related phenotypes found *in vivo* require compound deletions of related miRNAs within a particular miRNA family[50]. However, once coupled with a stress condition, such as γ-irradiation, dysregulation of *mir-237* can confer *in vivo*-related morphological defects, in addition to those already identified for *miR-34* and *let-7*[19,20].

Our results also indicate that *cel-mir-237* may function by regulating *jun-1*. Using sequence and conservation analysis, *jun-1* was predicted to be a target of *cel-mir-237* by two different algorithms[27,28]. In addition, it was previously reported that *jun-1* levels were upregulated when the miRNA biogenesis gene *dcr-1* was mutated, but did not change in *rde-1* or *rde-4* RNAi pathway-specific gene mutants[51]. Here, we have demonstrated an inverse relationship between *jun-1* and *cel-mir-237* levels not only in overexpressor and deletion mutants, but also in N2 animals following γ-irradiation treatment. Notably, following γ-irradiation, *jun-1* levels increased hours after *cel-mir-237* levels decreased. This result hints at a possible temporal correlation between *cel-mir-237* and *jun-1* post-γ-irradiation. Functionally, *cel-mir-237* overexpressor strains and *jun-1* loss-of-function mutant strains similarly exhibited higher sensitivities to γ-irradiation than N2 animals. Finally, in an epistatic study, *jun-1* loss-of-function and *mir-237(tm2238)* double mutants were more sensitive to γ-irradiation than N2 animals, which was similar to the phenotype of *jun-1* loss-of-function mutants, but opposite of that of *mir-237(tm2238*) mutants, indicating *jun1* and *cel-mir-237* are within the same genetic pathway. Taken together, these results are consistent with the hypothesis that *cel-mir-237* downregulates *jun-1* levels and that *jun1* expression is critically important in modulating cellular survival cues post-γ-irradiation.

Development of *C. elegans* vulval precursor cells depends upon signaling pathways that are also aberrantly activated in human breast cancer; therefore, we hypothesized that the mammalian *cel-mir-237* homologue, hsa-miR-125b, could promote a similar radiosensitizing phenotype. Indeed, MCF-7 and MDA-MB-231 breast cancer cells transfected with miR-125b mimic were more sensitive to γ-irradiation as compared to miR-Scr control treated cells. Our results are consistent with a study in oral squamous cell carcinoma cell lines in which forced expression of miR-125b, acting through the target gene, ICAM2, sensitized cells to X-ray-irradiation[52]. On the other hand, Tan *et al*. observed that overexpression of miR-125b promoted cell survival after UV-based irradiation through the downregulation of p38α[53]. These conflicting reports might be due to the fact that Tan *et al*. investigated the effects of UV-based irradiation, which promotes a different form of DNA damage, activating nucleotide excision repair rather than HR or NHEJ. Furthermore, Tan *et*

*al*. studied the acute effects of irradiation in miR-125b transfected cells, which was mainly a phenotype driven by apoptosis. However, our study utilized clonogenic assays to assess the long-term consequences of γ-irradiation in miR-125b expressing cells, which would capture both IR-induced apoptosis as well as delayed cell death.

The role of miR-125b in modulating irradiation-sensitivity in breast cancer is most likely a cell-context specific phenotype, given miR-125b itself has been described as a tumor suppressor in breast cancer[37,54–56], melanoma[57], and bladder cancer[58], but also as an oncogene in prostate cancer[59] and leukemia[60,61]. miR-125b has also been shown to promote stem cell-like properties in cholangiocarcinoma[62] and expand progenitor cell populations in acute megakaryoblastic leukemia[63]. Furthermore, miR-125b is significantly enriched in hair follicle stem cells and promotes initiation and malignant progression of skin tumors[45,64]. The diversity of miR-125b-induced phenotypes can largely be explained by the target mRNA genes that play an essential role in each of the aforementioned processes. As an example, miR-125b has been demonstrated to target genes in pathways involving cell proliferation, cell differentiation, and apoptosis including, *TP53*, *TDG*, *ERBB2/3*, *EPO*, pro-apoptotic genes such as *BAK1* and *PUMA*, and cell cycle regulators such as *CDC25C*[54,59,65–67].

In this study, we observed that the interaction between miR-125b and *JUN* controlled γ-irradiation sensitivity in MCF-7 and MDA-MB-231 breast cancer cells. The consequence of disrupting this regulatory network, either by forced miR-125b expression or inhibition of JUN activity during IR-induced stress, was increased senescence. We did not observe this phenomenon in normal HMEC cells. While it has been previously reported that miR-125b targets and reduces JUN expression during granulocyte differentiation[33,42] and promotes cellular senescence in melanoma[57], this is the first report identifying these two genes interacting within the same regulatory network to confer γ-irradiation sensitivity in breast cancer. We also identified miR-125b regulated genes involved in stress-response MAPK signaling, which are induced in cancer cells after γ-irradiation, presumably to promote cell survival. Certain breast cancer disease subtypes such as triple-negative breast cancer (TNBC), which are aggressive and have shorter intervals for locoregional recurrence, distant metastasis and disease-free survival[68–70], also harbor a heightened MAPK-gene signature. Future work will be required to determine if use of miR-125b as an adjuvant during IR treatment paradigms could enhance the radiosensitivity of tumor cells in these patient populations a well.

## Materials and Methods

### Nematode culture and strains, and gene bombardment

*C. elegans* were grown on nematode growth media (NGM) plates, fed the *E. coli* OP50 strain, and kept at either 20ºC or 23ºC, as described by Brenner[24]. Embryos from digested hermaphrodites hatched overnight in M9 without *E. coli* before starvation-arrested L1 nematodes were re-plated on OP50-seeded plates for syncronization[71,72]. N2 Bristol strain was used as the wild-type *C. elegans* strain. The *mir-237(tm2238)* strain was obtained from the National Bioresource Project for the nematode (Tokyo, Japan). Other miRNA-deletion mutants and *jun-1(gk551)* and *jun-1(gk557)* strains were obtained from the C. elegans

Genetics Center (CGC). Mutants were backcrossed to N2 6 times before being analyzed. The *unc-119(ed3);[Cbr unc-119::mir-237]#7* and *unc-119(ed3);[Cbr unc-119::mir-237]#44* strains were generated via micro-particle bombardment[73,74] of *Cbr unc-119::mir-237* constructs into the *C. elegans unc-119(ed3)* starvation-induced lethal reporter system[75]. Primers for cloning and characterization are shown in Table S4. Animals were assessed for stable integration, copy number, and levels of integrated gene expression. *jun-1(gk551);mir-237(tm2238)*, and *jun-1(gk557);mir-237(tm2238)* strains were generated by genetic crossing of each of the two indicated strains. Male nematodes were only used for genetic crossing; all animals examined in the radiation treatment experiments were hermaphrodites.

## Determination of radiation treatment dose response

To minimize cell-cycle dependent variation in irradiation sensitivity experiments, synchronized *C. elegans* strains were examined at a fixed radiation dosage using a $Cesium^{137}$ source to determine peak radioresistance post-hatching as discussed in[22]. The time-point showing greatest radioresistance was the point at which the greatest proportion of animals had wild-type vulvae[22]. All experiments were performed twice and radioresistance peak times are shown in Table S5.

Animals were synchronized and placed on OP50-NGM plates for the duration of time as determined by the radioresistance peak assay. Animals were placed in a 15-ml conical tube with OP50-seeded NGM and irradiated at 0-400Gy. Animals were scored for vulval malformations as adults[22]. Normal vulval structures were scored as a wild-type (WT) phenotype; conversely, a protruding vulval (Pvl) or the absence of a vulva structure (Vul) was categorized as a mutant (Mut) phenotype. Dose curves are presented as ratios of animals with WT:Mut vulva. For each dose-response, one data-point represents 3 biological replicates each containing ~150-300 animals (averages of 245.35 animals per replicate for Fig. 1A; 215.80 for Fig. 1C; 174.33 for Fig. 2D; and 190.27 for Fig. 2E). Statistical analysis was done by 2-tailed paired t-test. All strains were normalized to 0Gy data-points.

## Cell lines and transfections

MCF-7 and MDA-MB-231 cells were obtained from the American Type Culture Collection (ATCC), and cultured at 37ºC with 5% $CO_2$ in RPMI supplemented with 10% FBS and 1% penicillin/streptomycin. HMECs were maintained as per manufacture's protocol (Life Technologies). All experiments were performed within 1-2 years upon receipt of cells, and characterized by STR analysis via ATCC. Cell lines were tested for mycoplasma via the Lonza MycoAlert™ Detection Kit. For RNA-based functional experiments, *mir*Vana mimics and validated Silencer Select siRNAs (Life Technologies) were transfected into $5\times10^4$ cells using DharmaFECT 1 (GE Healthcare Dharmacon), as per manufacture's protocol.

## Plasmids and generation of stable cell lines

To generate the stable c-JUN-ORF-IRES-GFP MDA-MB-231 line, HEK-293T cells were co-transfected with pCMV-VSVG and pCMV-dR8.2 (gag/pol) helper constructs (Addgene) along with a pMIEG3-c-Jun expression plasmid (Addgene) using Fugene 6 (Promega). A

pMIEG3-empty control construct was also generated by excising the c-Jun sequence via NotI / XhoI endonuclease digestion. Retrovirus was produced using The RNAi Consortium protocols (www.broadinstitute.org/rnai/public). Stable transductants were double sorted for GFP on a BD FACS Aria flow cytometer.

## Clonogenic assays

Unless otherwise indicated, $1\times10^5$ cells were seeded into 12-well plates and transfected with 30nM miR-125b mimic or negative control mimic, 15nM miR-125b inhibitor or negative control inhibitor, and 15nM si-Jun or scrambled siRNA (Life Technologies) in antibiotic-free RPMI media. 24hrs post-transfection cells were re-seeded into 6-well plates for expansion. In some experiments cells were pre-treated with Tanshinone IIA. 72hrs later cells were irradiated at 0-6Gy. Cells were immediately seeded into 6-well plates at ~100–900 cells per well, depending upon γ-irradiation condition from the lowest number of cells (100-200) at 0Gy, (275) at 2Gy, (400) at 4Gy, to the highest (900) at 6 Gy in order to produce colonies with clearly defined borders and minimal overlapping. After 10 days of undisturbed growth, colonies were fixed, stained with crystal violet, and counted on a dissection scope (Zeiss). Plating efficiency and surviving fraction were calculated from technical quadruplicates of each γ-irradiation dose and miRNA condition. Experiments were performed a minimum of three times. Statistical significance was evaluated by two-way ANOVA (two-tailed) of the data for each transfection or drug treatment across all doses.

## RNA-based functional experiments

For cytotoxicity assessment and development of $IC_{50}$ curves, Sulforhodamine Blue (SRB) assays were performed as previously described[36]. Briefly, transfected or drug treated cells were seeded into 24-well plates, HMECs were additionally treated with γ-irradiation, and at indicated times cells were fixed, stained, and dye intensity quantified. Additionally, transfected cells underwent γ-irradiation treatment and were analyzed for presence of apoptosis by the Annexin V Apoptosis Detection Kit (BD Pharmigen), presence of senescence by the SA-β-Galactosidase Staining Kit (Cell Signaling Technology)[36,76], and for cell cycle analysis as previously described[36]. Unless otherwise stated, data was made relative to the initial time point for each treatment condition and presented as the average of at least two independent experiments ±/- SD. *p-values* were calculated by two-way ANOVA.

For DNA damage assays, transfected cells were treated with either 0 or 4Gy γ-irradiation, embedded in low-melt agarose, and spread onto slides for alkaline lysis and electrophoresis as described previously[77]. Individual cells were scored from 0 to 4, where 0=no DNA damage and 4=extensive tailing indicative of severe DNA damage. Cells were scored from 10 fields per slide with 3 replicates for each condition. *p-values* were calculated by Fisher's exact test.

## RNA isolation and qRT-PCR

*C. elegans* were synchronized and sample collections occurred at the indicated time post-irradiation. 3600 animals were lysed for RNA extraction using the mirVana miRNA Isolation Kit. Cell lines were lysed in TRIzol. Total RNA was treated with Turbo DNase. For mRNA analysis, cDNA synthesis was performed using SuperScript III with oligo dT

primers. 2.5ng of input cDNA was used for SYBR Green-based real-time PCR. Gene expression was normalized to RPL19 for mammalian cells, and *pmp-3*[78] for *C. elegans*.

For *C. elegans* miRNA analysis, qRT-PCR was performed using the TaqMan® miRNA system as per manufacturer's instructions, and gene expression was normalized to U18. For mammalian miRNA analysis, qRT-PCR was performed using the miScript II system (Qiagen). MiRNA expression was normalized to RNU6B. qPCR reactions were analyzed on a Roche LightCycler 480 instrument. Primers used in this study are listed in Table S6. All experiments include 3 biological replicates unless otherwise stated in the figure legends.

For qPCR arrays, MCF-7 and MDA-MB-231 breast cancer cells were transfected with 15nM miR-125b or miR-Scr control in duplicate and harvested for RNA 72 hours post-transfection. Lysates were converted to cDNA using the RT$^2$ First Strand Kit, and run on RT$^2$ Profiler Human MAPK Signaling PCR Arrays (Qiagen) measuring expression of 84 genes in this pathway. Gene expression was normalized using the geometric mean of *GAPDH*, *HPRT1*, and *RPLP0* expression, and was then further processed for miRNA target-enrichment analysis. All genes that were 2-fold downregulated by miR-125b and 2-fold upregulated after γ-irradiation treatment were considered candidates for a miR-125b-γ-irradiation gene signature. Genes that were strongly elevated after γ-irradiation in both cells lines, yet were downregulated by miR-125b are shown in Table S3.

## Western Blotting

Cell lines at various times post-transfection or after γ-irradiation were collected and lysed in radioimmunoprecipitation assay buffer (Thermo Scientific) supplemented with protease and phosphatase inhibitors (Roche) as previously described[36]. 20μg protein was resolved onto 4-20% mini-PROTEAN TGX gels (Bio-Rad), and transferred to PVDF membranes. Primary antibodies were used to detect pSer73-JUN (1:1000, Cell Signaling Technology, #3270), c-JUN (1:1000, Cell Signaling Technology, #9165), and β-actin (1:1000, Cell Signaling Technology, #4970). Following incubation with anti-rabbit IgG horseradish peroxidase-conjugated secondary antibodies (1:10,000, Santa Cruz, #2030), expression was detected via Clarity Western ECL (BioRad) and chemiluminescent film (Denville Scientific). Band intensities were quantified using NIH Image J software.

## Bioinformatic analysis and miRNA target prediction

Predicted miRNA gene targets were acquired from three published databases: miRanda[26,27], TargetScanWorm[28,29], and mirWIP[30]. Bioinformatic analysis of putative miR-125b targets were performed using TargetScan[7]. All predicted targets were further selected based on, *1)* being predicted by more than one database (Table S1) and *2)* having known or predicted functions that are involved in DNA repair and DNA damage response[31], cell survival and cell proliferation, AP-1 complex formation, or were genes from a recent RNAi screen identifying radio-sensitizers in *C. elegans*[32]. Overlapping miRNA-targets with irradiation-response genes, or to genes changed after miR-125b transfection, or γ-irradiation treatment was performed using GeneVenn.

### Statistical analysis

Statistical analysis was achieved by 2-tailed paired t-test for vulval radiation sensitivity assay, Fisher's exact test for DNA damage comet assay, 2-tailed Student's t-test for gene expression analysis by qRT-PCR, and 2-way ANOVA for clonogenic assays, Annexin V staining assay, and SA-β-gal assay. All graphs show means ± S.D. Additionally for qRT-PCR data, means and S.D. were calculated at the ddCt level before being converted to fold changes as presented in the graphs[79].

## Supplementary Material

Refer to Web version on PubMed Central for supplementary material.

## Acknowledgments

We thank Geoffrey Lyon, Yale Cell Sorter Core Facility, for assistance with FACS sorting and analysis, the Yale Cesium Irradiator Shared Resource for use of γ-irradiator, Valerie Horsley for use of imaging equipment, and to Shirin Bahmanyar for providing space and making equipment available for these studies. We thank Alan Jiao and Catherine O. Adams for critical reading of this manuscript. Nematode strains used in this work were provided by the C. elegans Genetics Center, which is funded by the National Institutes of Health National Center for Research Resources.

**Grant Support:** This work was supported by grants to F.J.S. and J.B.W from the NIH (R01 CA157749 and R01 CA131301). B.D.A. was supported by a training grant (5T32 HG003198-10).

## References

1. Shrivastav M, De Haro LP, Nickoloff JA. Regulation of DNA double-strand break repair pathway choice. Cell Res. 2008; 18:134–47. [PubMed: 18157161]
2. Krejci L, Altmannova V, Spirek M, Zhao X. Homologous recombination and its regulation. Nucleic Acids Res. 2012; 40:5795–818. [PubMed: 22467216]
3. Lieber MR. The mechanism of double-strand DNA break repair by the nonhomologous DNA end-joining pathway. Annu Rev Biochem. 2010; 79:181–211. [PubMed: 20192759]
4. Zhang C, Wang S, Israel HP, Yan SX, Horowitz DP, Crockford S, et al. Higher locoregional recurrence rate for triple-negative breast cancer following neoadjuvant chemotherapy, surgery and radiotherapy. Springerplus. 2015; 4:386. [PubMed: 26240784]
5. Bartel DP. MicroRNAs: genomics, biogenesis, mechanism, and function. Cell. 2004; 116:281–97. [PubMed: 14744438]
6. Ambros V. The functions of animal microRNAs. Nature. 2004; 431:350–5. [PubMed: 15372042]
7. Lewis BP, Burge CB, Bartel DP. Conserved seed pairing, often flanked by adenosines, indicates that thousands of human genes are microRNA targets. Cell. 2005; 120:15–20. [PubMed: 15652477]
8. Bartel DP. MicroRNAs: target recognition and regulatory functions. Cell. 2009; 136:215–33. [PubMed: 19167326]
9. Adams BD, Kasinski AL, Slack FJ. Aberrant Regulation and Function of MicroRNAs in Cancer. Curr Biol. 2014; 24:R762–R776. [PubMed: 25137592]
10. Esquela-Kerscher A, Slack FJ. Oncomirs - microRNAs with a role in cancer. Nat Rev Cancer. 2006; 6:259–69. [PubMed: 16557279]
11. Farazi, Ta, Spitzer, JI., Morozov, P., Tuschl, T. miRNAs in human cancer. J Pathol. 2011; 223:102–15. [PubMed: 21125669]
12. Macfarlane LA, Murphy PR. MicroRNA: Biogenesis, Function and Role in Cancer. Curr Genomics. 2010; 11:537–61. [PubMed: 21532838]
13. Garofalo M, Croce CM. MicroRNAs as therapeutic targets in chemoresistance. Drug Resist Updat. 2013; 16:47–59. [PubMed: 23757365]

14. Cheng CJ, Bahal R, Babar IA, Pincus Z, Barrera F, Liu C, et al. MicroRNA silencing for cancer therapy targeted to the tumour microenvironment. Nature. 2015; 518:107–10. [PubMed: 25409146]
15. Peter ME. Targeting of mRNAs by multiple miRNAs: the next step. Oncogene. 2010; 29:2161–4. [PubMed: 20190803]
16. Kai ZS, Pasquinelli AE. MicroRNA assassins: factors that regulate the disappearance of miRNAs. Nat Struct Mol Biol. 2010; 17:5–10. [PubMed: 20051982]
17. Misso G, Teresa M, Martino D, Rosa G De, Farooqi AA, Lombardi A, et al. Mir-34: A New Weapon Against Cancer? Mol Ther Nucleic Acids. 2014; 3:e194.
18. Babar IA, Czochor J, Steinmetz A, Weidhaas JB, Glazer PM, Slack FJ. Inhibition of hypoxia-induced miR-155 radiosensitizes hypoxic lung cancer cells. Cancer Biol Ther. 2011; 12
19. Kato M, Paranjape T, Müller RU, Ullrich R, Nallur S, Gillespie E, et al. The mir-34 microRNA is required for the DNA damage response in vivo in C. elegans and in vitro in human breast cancer cells Oncogene. 2009; 28:2419–24. [PubMed: 19421141]
20. Weidhaas JB, Babar I, Nallur SM, Trang P, Roush S, Boehm M, et al. MicroRNAs as potential agents to alter resistance to cytotoxic anticancer therapy. Cancer Res. 2007; 67:11111–6. [PubMed: 18056433]
21. Metheetrairut C, Slack FJ. MicroRNAs in the ionizing radiation response and in radiotherapy. Curr Opin Genet Dev. 2013; 23:12–9. [PubMed: 23453900]
22. Weidhaas JB, Eisenmann DM, Holub JM, Nallur SV. A Caenorhabditis elegans tissue model of radiation-induced reproductive cell death. Proc Natl Acad Sci U S A. 2006; 103:9946–51. [PubMed: 16788064]
23. Brown JM, Wilson G. Apoptosis genes and resistance to cancer therapy: what does the experimental and clinical data tell us? Cancer Biol Ther. 2:477–90.
24. Brenner S. The genetics of Caenorhabditis elegans. Genetics. 1974; 77:71–94. [PubMed: 4366476]
25. Sulston JE, Horvitz HR. Post-embryonic cell lineages of the nematode, Caenorhabditis elegans. Dev Biol. 1977; 56:110–156. [PubMed: 838129]
26. Betel D, Koppal A, Agius P. Comprehensive modeling of microRNA targets predicts functional non-conserved and non-canonical sites. Genome Biol. 2010; 11:R90. [PubMed: 20799968]
27. Betel D, Wilson M, Gabow A. The microRNA. org resource: targets and expression. Nucleic acids. 2008; 36doi: 10.1093/nar/gkm995
28. Friedman R, Farh K. Most mammalian mRNAs are conserved targets of microRNAs. Genome Res. 2009; 19:92–105. [PubMed: 18955434]
29. Jan C, Friedman R, Ruby J, Bartel D. Formation, regulation and evolution of Caenorhabditis elegans 3 UTRs. Nature. 2011; 469:97–101. [PubMed: 21085120]
30. Hammell M, Long D, Zhang L, Lee A. mirWIP: microRNA target prediction based on microRNA-containing ribonucleoprotein–enriched transcripts. Nat. 2008; 5:813–819.
31. O'Neil N, Rose A. DNA repair. WormBook. 2006:1–12.
32. van Haaften G, Romeijn R, Pothof J, Koole W, Mullenders LHF, Pastink A, et al. Identification of Conserved Pathways of DNA-Damage Response and Radiation Protection by Genome-Wide RNAi. Curr Biol. 2006; 16:1344–1350. [PubMed: 16824923]
33. Surdziel E, Cabanski M, Dallmann I, Lyszkiewicz M, Krueger A, Ganser A, et al. Enforced expression of miR-125b affects myelopoiesis by targeting multiple signaling pathways. Blood. 2011; 117:4338–4348. [PubMed: 21368288]
34. Feng H, Craig HL, Hope IA. Expression pattern analysis of regulatory transcription factors in Caenorhabditis elegans. Methods Mol Biol. 2012; 786:21–50. [PubMed: 21938618]
35. Esquela-Kerscher A, Johnson SM, Bai L, Saito K, Partridge J, Reinert KL, et al. Post-embryonic expression of C. elegans microRNAs belonging to the lin-4 let-7 families in the hypodermis and the reproductive system. Dev Dyn. 2005; 234:868–877. [PubMed: 16217741]
36. Adams BD, Wali VB, Cheng CJ, Inukai S, Booth CJ, Agarwal S, et al. miR-34a Silences c-SRC to Attenuate Tumor Growth in Triple Negative Breast Cancer. Cancer Res. 2015; doi: 10.1158/0008-5472.CAN-15-2321

37. Zhang Y, Yan LX, Wu QN, Du ZM, Chen J, Liao DZ, et al. miR-125b is methylated and functions as a tumor suppressor by regulating the ETS1 proto-oncogene in human invasive breast cancer. Cancer Res. 2011; 71:3552–62. [PubMed: 21444677]
38. Wu D, Ding J, Wang L, Pan H, Zhou Z, Zhou J, et al. microRNA-125b inhibits cell migration and invasion by targeting matrix metallopeptidase 13 in bladder cancer. Oncol Lett. 2013; 5:829–834. [PubMed: 23425975]
39. Tang J, Ahmad A, Sarkar FH. The Role of MicroRNAs in Breast Cancer Migration, Invasion and Metastasis. Int J Mol Sci. 2012; 13:13414–37. [PubMed: 23202960]
40. Iliakis G. Cell cycle regulation in irradiated and nonirradiated cells. Semin Oncol. 1997; 24:602–615. [PubMed: 9422257]
41. Bernhard EJ, Maity a, Muschel RJ, McKenna WG. Effects of ionizing radiation on cell cycle progression. A review Radiat Env Biophys. 1995; 34:79–83. [PubMed: 7652155]
42. Kappelmann M, Kuphal S, Meister G, Vardimon L, Bosserhoff AK. MicroRNA miR-125b controls melanoma progression by direct regulation of c-Jun protein expression. Oncogene. 2013; 32:2984–91. [PubMed: 22797068]
43. Mechta-Grigoriou F, Gerald D, Yaniv M. The mammalian Jun proteins: redundancy and specificity. Oncogene. 2001; 20:2378–89. [PubMed: 11402334]
44. Wu L, Fan J, Belasco JG. MicroRNAs direct rapid deadenylation of mRNA. Proc Natl Acad Sci U S A. 2006; 103:4034–4039. [PubMed: 16495412]
45. Zhang L, Ge Y, Fuchs E. miR-125b can enhance skin tumor initiation and promote malignant progression by repressing differentiation and prolonging cell survival. Genes Dev. 2014; 28:2532–46. [PubMed: 25403182]
46. Ambros V, Lee RC, Lavanway A, Williams PT, Jewell D. MicroRNAs and other tiny endogenous RNAs in C. Elegans Curr Biol. 2003; 13:1317–1323. [PubMed: 12906792]
47. Lim LP, Lau NC, Weinstein EG, Abdelhakim A, Yekta S, Rhoades MW, et al. The microRNAs of Caenorhabditis elegans. Genes Dev. 2003; 17:991–1008. [PubMed: 12672692]
48. Lee RC, Feinbaum RL, Ambros V. The C. elegans heterochronic gene lin-4 encodes small RNAs with antisense complementarity to lin-14. Cell. 1993; 75:843–854. [PubMed: 8252621]
49. Miska, Ea, Alvarez-Saavedra, E., Abbott, AL., Lau, NC., Hellman, AB., McGonagle, SM., et al. Most Caenorhabditis elegans microRNAs are individually not essential for development or viability. PLoS Genet. 2007; 3:2395–2403.
50. Song R, Walentek P, Sponer N, Klimke A, Lee JS, Dixon G, et al. miR-34/449 miRNAs are required for motile ciliogenesis by repressing cp110. Nature. 2014; 510:115–120. [PubMed: 24899310]
51. Welker NC, Habig JW, Bass BL. Genes misregulated in C. elegans deficient in Dicer, RDE-4, or RDE-1 are enriched for innate immunity genes. RNA. 2007; 13:1090–1102. [PubMed: 17526642]
52. Shiiba M, Shinozuka K, Saito K, Fushimi K, Kasamatsu a, Ogawara K, et al. MicroRNA-125b regulates proliferation and radioresistance of oral squamous cell carcinoma. Br J Cancer. 2013; 108:1817–21. [PubMed: 23591197]
53. Tan G, Niu J, Shi Y, Ouyang H, Wu ZH. NF-kappaB-dependent microRNA-125b up-regulation promotes cell survival by targeting p38alpha upon ultraviolet radiation. J BiolChem. 2012; 287:33036–33047.
54. Scott GK, Goga A, Bhaumik D, Berger CE, Sullivan CS, Benz CC. Coordinate suppression of ERBB2 and ERBB3 by enforced expression of micro-RNA miR-125a or miR-125b. J Biol Chem. 2007; 282:1479–1486. [PubMed: 17110380]
55. Rajabi H, Jin C, Ahmad R, McClary AC, Joshi MD, Kufe D. Mucin 1 oncoprotein expression is suppressed by the miR-125b oncomir. Genes and Cancer. 2010; 1:62–68. [PubMed: 20729973]
56. Feliciano A, Castellvi J, Artero-Castro A, Leal JA, Romagosa C, Hernández-Losa J, et al. miR-125b acts as a tumor suppressor in breast tumorigenesis via its novel direct targets ENPEP, CK2-α, CCNJ, and MEGF9. PLoS One. 2013; 8:e76247. [PubMed: 24098452]
57. Nyholm AM, Lerche CM, Manfé V, Biskup E, Johansen P, Morling N, et al. miR-125b induces cellular senescence in malignant melanoma. BMC Dermatol. 2014; 14:8. [PubMed: 24762088]
58. Huang L, Luo J, Cai Q, Pan Q, Zeng H, Guo Z, et al. MicroRNA-125b suppresses the development of bladder cancer by targeting E2F3. Int J Cancer. 2011; 128:1758–69. [PubMed: 20549700]

59. Shi XB, Xue L, Ma AH, Tepper CG, Kung HJ, White RW, deVere. miR-125b promotes growth of prostate cancer xenograft tumor through targeting pro-apoptotic genes. Prostate. 2011; 71:538–49. [PubMed: 20886540]
60. Gefen N, Binder V, Zaliova M, Linka Y, Morrow M, Novosel A, et al. Hsa-mir-125b-2 is highly expressed in childhood ETV6/RUNX1 (TEL/AML1) leukemias and confers survival advantage to growth inhibitory signals independent of p53. Leukemia. 2010; 24:89–96. [PubMed: 19890372]
61. Puissegur MP, Eichner R, Quelen C, Coyaud E, Mari B, Lebrigand K, et al. B-cell regulator of immunoglobulin heavy-chain transcription (Bright)/ARID3a is a direct target of the oncomir microRNA-125b in progenitor B-cells. Leukemia. 2012; 26:2224–2232. [PubMed: 22469780]
62. Lin KY, Ye H, Han BW, Wang WT, Wei PP, He B, et al. Genome-wide screen identified let-7c/miR-99a/miR-125b regulating tumor progression and stem-like properties in cholangiocarcinoma. Oncogene. 2015; doi: 10.1038/onc.2015.396
63. Emmrich S, Rasche M, Schöning J, Reimer C, Keihani S, Maroz A, et al. miR-99a/100~125b tricistrons regulate hematopoietic stem and progenitor cell homeostasis by shifting the balance between TGFβ and Wnt signaling. Genes Dev. 2014; 28:858–74. [PubMed: 24736844]
64. Zhang L, Stokes N, Polak L, Fuchs E. Specific microRNAs are preferentially expressed by skin stem cells to balance self-renewal and early lineage commitment. Cell Stem Cell. 2011; 8:294–308. [PubMed: 21362569]
65. Ferracin M, Bassi C, Pedriali M, Pagotto S, D'Abundo L, Zagatti B, et al. miR-125b targets erythropoietin and its receptor and their expression correlates with metastatic potential and ERBB2/HER2 expression. Mol Cancer. 2013; 12:130. [PubMed: 24165569]
66. Le MTN, Shyh-Chang N, Khaw SL, Chin L, Teh C, Tay J, et al. Conserved regulation of p53 network dosage by microRNA-125b occurs through evolving miRNA-target gene pairs. PLoS Genet. 2011; 7:1–11.
67. Le MTN, Teh C, Shyh-Chang N, Xie H, Zhou B, Korzh V, et al. MicroRNA-125b is a novel negative regulator of p53. Genes Dev. 2009; 23:862–876. [PubMed: 19293287]
68. Lowery AJ, Kell MR, Glynn RW, Kerin MJ, Sweeney KJ. Locoregional recurrence after breast cancer surgery: A systematic review by receptor phenotype. Breast Cancer Res Treat. 2012; 133:831–841. [PubMed: 22147079]
69. Zaky SS, Lund M, May KA, Godette KD, Beitler JJ, Holmes LR, et al. The negative effect of triple-negative breast cancer on outcome after breast-conserving therapy. Ann Surg Oncol. 2011; 18:2858–2865. [PubMed: 21442346]
70. Dent R, Trudeau M, Pritchard KI, Hanna WM, Kahn HK, Sawka CA, et al. Triple-negative breast cancer: clinical features and patterns of recurrence. Clin Cancer Res. 2007; 13:4429–34. [PubMed: 17671126]
71. Stiernagle T. Maintenance of C. elegans. WormBook. 2006:1–11.
72. Girard LR, Fiedler TJ, Harris TW, Carvalho F, Antoshechkin I, Han M, et al. WormBook: The online review of Caenorhabditis elegans biology. Nucleic Acids Res. 2007; 35doi: 10.1093/nar/gkl894
73. Isik M, Berezikov E. Biolistic transformation of Caenorhabditis elegans. Methods Mol Biol. 2013; 940:77–86. [PubMed: 23104335]
74. Praitis V, Casey E, Collar D, Austin J. Creation of low-copy integrated transgenic lines in Caenorhabditis elegans. Genetics. 2001; 157:1217–26. [PubMed: 11238406]
75. Zhao Z, Flibotte S, Murray JI, Blick D, Boyle TJ, Gupta B, et al. New tools for investigating the comparative biology of Caenorhabditis briggsae and C. elegans Genetics. 2010; 184:853–63. [PubMed: 20008572]
76. Dimri GP, Lee X, Basile G, Acosta M, Scott G, Roskelley C, et al. A biomarker that identifies senescent human cells in culture and in aging skin in vivo. Proc Natl Acad Sci U S A. 1995; 92:9363–7. [PubMed: 7568133]
77. Olive PL, Banáth JP. The comet assay: a method to measure DNA damage in individual cells. Nat Protoc. 2006; 1:23–9. [PubMed: 17406208]
78. Hoogewijs D, Houthoofd K, Matthijssens F, Vandesompele J, Vanfleteren JR. Selection and validation of a set of reliable reference genes for quantitative sod gene expression analysis in C. elegans. BMC Mol Biol. 2008; 9:9. [PubMed: 18211699]

79. Livak KJ, Schmittgen TD. Analysis of Relative Gene Expression Data Using Real-Time Quantitative PCR and the 2-ΔΔCT Method. Methods. 2001; 25:402–408. [PubMed: 11846609]

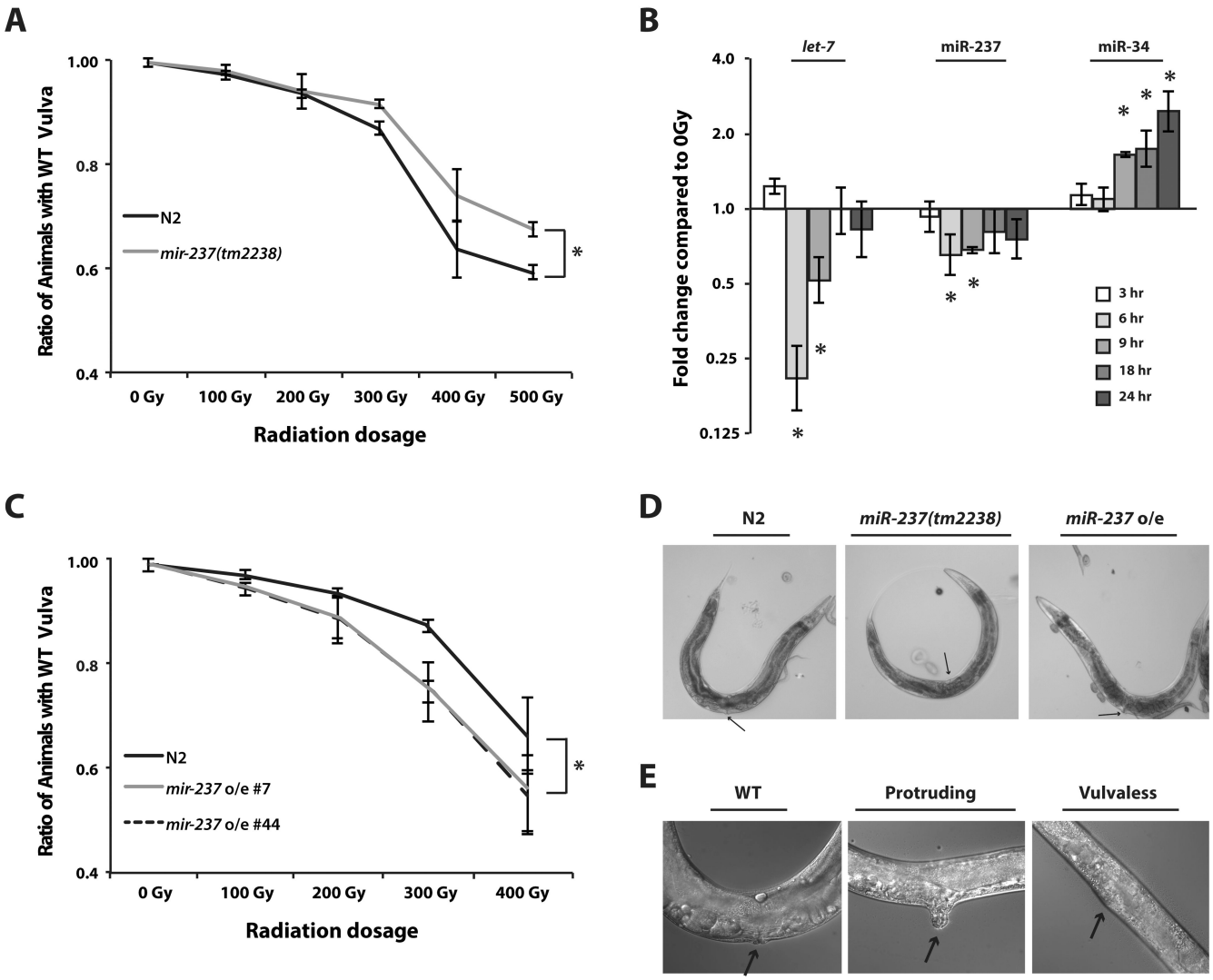


**Figure 1. cel-mir-237 modulates γ-irradiation response in C. elegans**

**(A)** *mir-237(tm2238)* deletion mutants exhibited higher WT vulval phenotypes than N2 animals, especially at higher γ-irradiation dosages, * *p-value* <0.005. **(B)** *cel-mir-237* was downregulated after IR. N2 animals were treated with 400Gy γ-irradiation or 0Gy mock treatment. The levels of expression were determined by qRT-PCR from samples collected at 3, 6, 9, 18, and 24hrs following irradiation of synchronized animals, * *p-value* <0.05. **(C)** Two *cel-mir-237* overexpressor lines (*mir-237* o/e #7 and #44) harbored higher frequencies of abnormal vulval phenotypes than N2 animals post- γ-irradiation, * *p-value* <0.001. **(D)** Representative images of N2, *mir-237(tm2238)*, and *mir-237* o/e lines, indicating a lack of gross morphological phenotypes prior to IR, → indicates location of the vulva. **(E)** Images representing the scoreable vulval defects in *C. elegans* post-γ-irradiation.

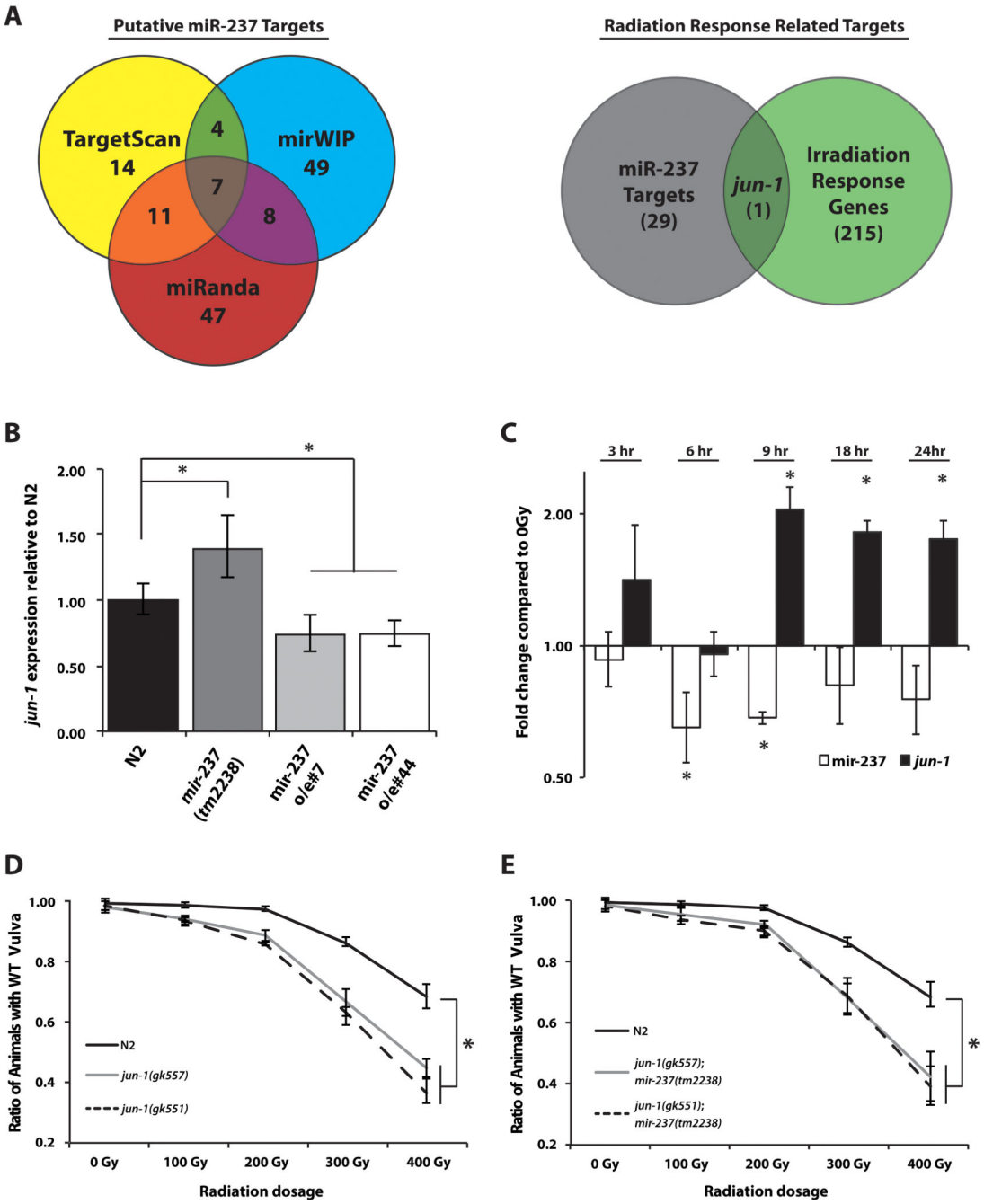


**Figure 2. jun-1 protects C. elegans from γ-irradiation**

**(A)** Venn diagram depicting overlap of putative *cel-mir-237* targets predicted by each miRNA targeting algorithms; TargetScanWorm[28,29], mirWIP[30], and miRanda[26,27] (*left panel*). Venn diagram depicting an overlapping set of predicted *cel-mir-237* targets with a curated irradiation response gene-set (*right panel*). **(B)** *jun-1* expression level is negatively correlated with *cel-mir-237* level. The levels of *jun-1* increased in *mir-237(tm2238)* deletion mutants, but decreased in *cel-mir-237* o/e #7 and #44 lines, as compared to N2 animals. The levels of expression of *jun-1* in all three mutant strains are significantly different from that of

N2 animals, * *p-value* <0.05. **(C)** The levels of *jun-1* in irradiated N2 animals as analyzed by qRT-PCR. *jun-1* increased at 9, 18, and 24hrs post-γ-irradiation, in comparison to the 0Gy mock-treated group collected at respective time points. This increase occurred only after the decrease in *cel-mir-237* levels at 6-9 hours post-γ-irradiation, * *p-value* <0.05. **(D)** *jun-1* mutants and **(E)** *mir-237;jun-1* double mutants are more sensitive to γ-irradiation. *jun-1(gk551)*, *jun-1(gk557)*, *jun-1(gk551);mir-237(tm2238)*, and *jun-1(gk557);mir-237(tm2238)* animals all exhibited significantly lower ratio of WT vulva than N2 animals, * *p-value* <0.001.

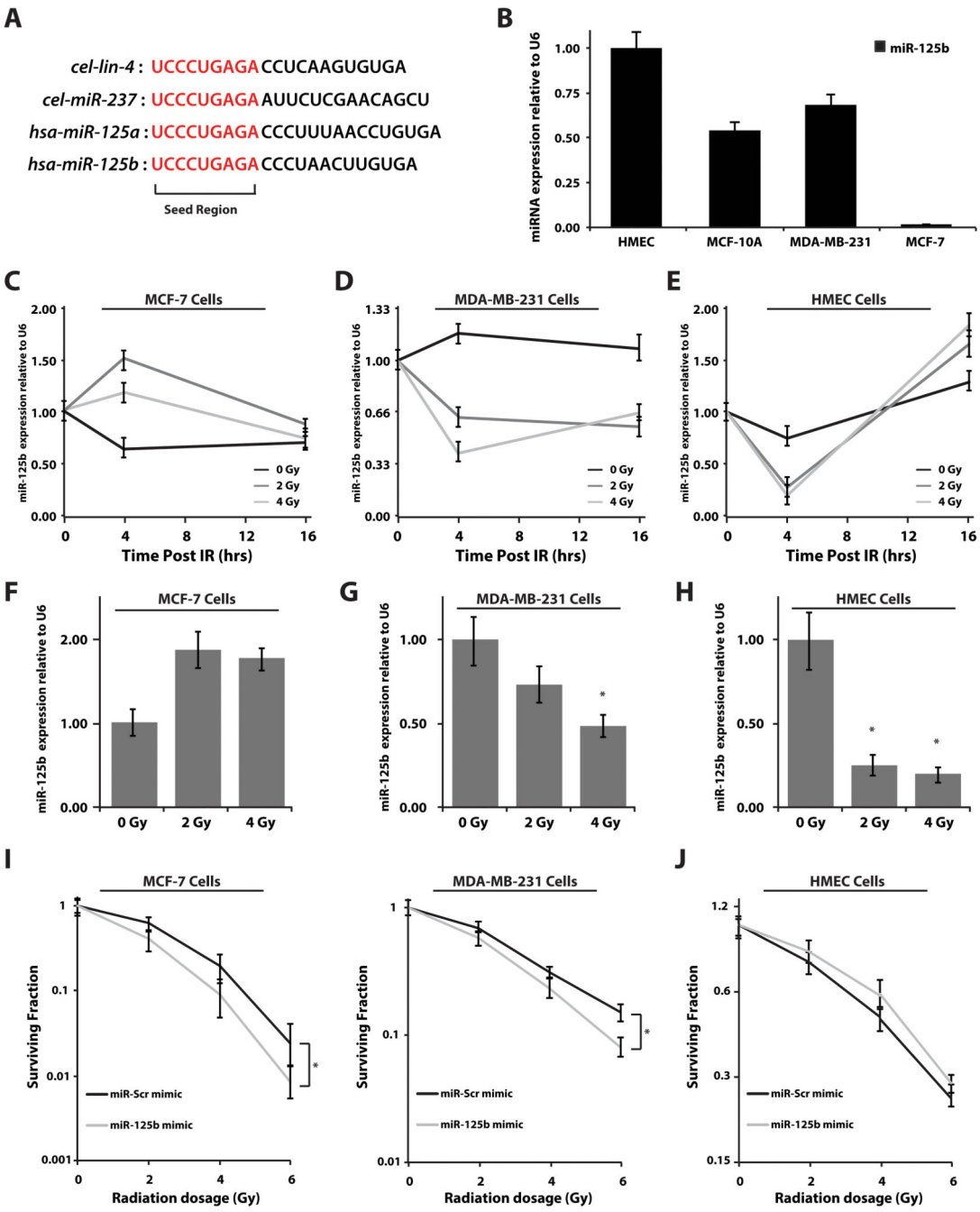


**Figure 3. hsa-miR-125b levels decrease following IR, and promotes γ-irradiation sensitivity**

**(A)** Mature *cel-lin-4*, *cel-mir-237*, hsa-miR-125a, and hsa-miR-125b share seed sequence (bases 2 – 8/9) and similar sequences at the 3′ end. **(B)** qRT-PCR analysis of miR-125b levels in normal HMEC and MCF-10A cells as compared to MDA-MB-231 and MCF-7 breast cancer cells. **(C)** MCF-7 and **(D)** MDA-MB-231 breast cancer cells, as well as **(E)** normal HMEC cells were irradiated at 0-4Gy and then collected for qRT-PCR analysis 0-16hrs later. Time-course indicates endogenous miR-125b levels respond rapidly post-γ-irradiation. (**F–H**) Assessment of miR-125b levels 4hrs post-γ-irradiation, * *p-value* <0.01.

**(I)** Analysis of clonogenic assays on MCF-7 and MDA-MB-231 cells 10 days following γ-irradiation. Cell lines transfected with miR-125b mimic 72hrs prior to γ-irradiation harbored lower colony forming potential than those transfected with miR-Scr control. For MCF-7 and MDA-MB-231 cells, *p-values* were <0.001 and <0.01, respectively, as determined by 2-way ANOVA. **(J)** For HMEC cells, surviving fraction was determined by Trypan Blue counts 6 days post-γ-irradiation. No significant difference was observed between miR-125b vs. miR-Scr transfected cells.

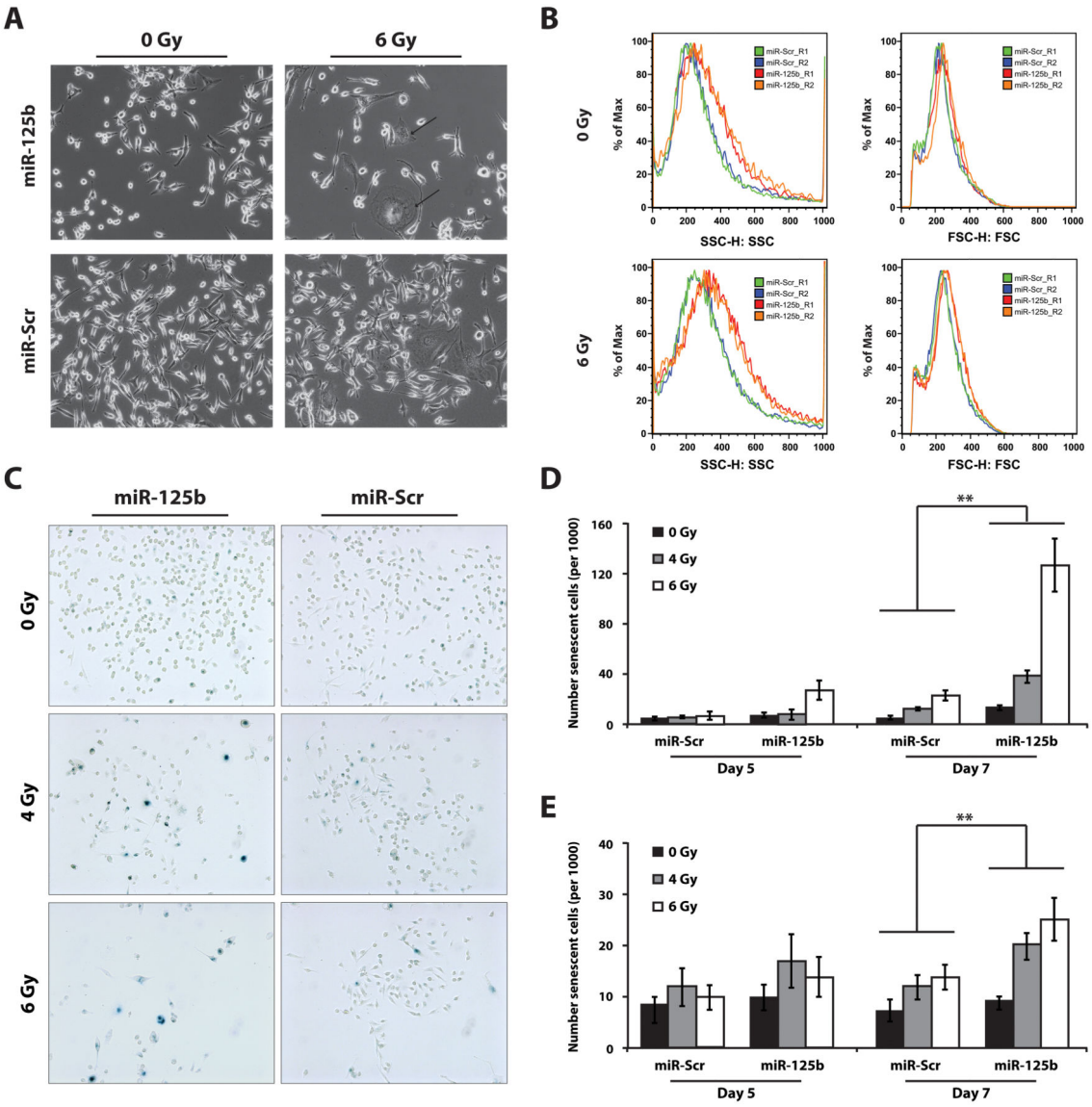


**Figure 4. hsa-miR-125b promotes γ-irradiation-induced senescence**

**(A)** Representative phase contrast images of MDA-MB-231 cells transfected with miR-125b or miR-Scr control mimic plus 0 or 6Gy γ-irradiation treatment. Fewer cells are observable in miR-125b vs. miR-Scr treated cells, however increased frequency of flat cells with extended cytoplasm emerged in miR-125b and 6Gy co-treated cells, →. **(B)** FACS analysis of MDA-MB-231 cells indicating heightened granularity in miR-125b transfected cells, and a further intensity of granularity upon addition of 6Gy γ-irradiation, *left panels*. Overall cell size was not dramatically different under any of these conditions, *right panels*. R1/R2 indicates two different cell replicates. **(C)** Representative images from SA-β-gal assays indicating MDA-MB-231 cells treated with both 30nM miR-125b and γ-irradiation promoted senescence. **(D)** Quantification of the MDA-MB-231 experiment at days 5 and 7, ** *p-value* <0.0001 by 2-way ANOVA. **(E)** Quantification of SA-β-gal experiment in MCF-7 cells, ** *p-value* <0.01.

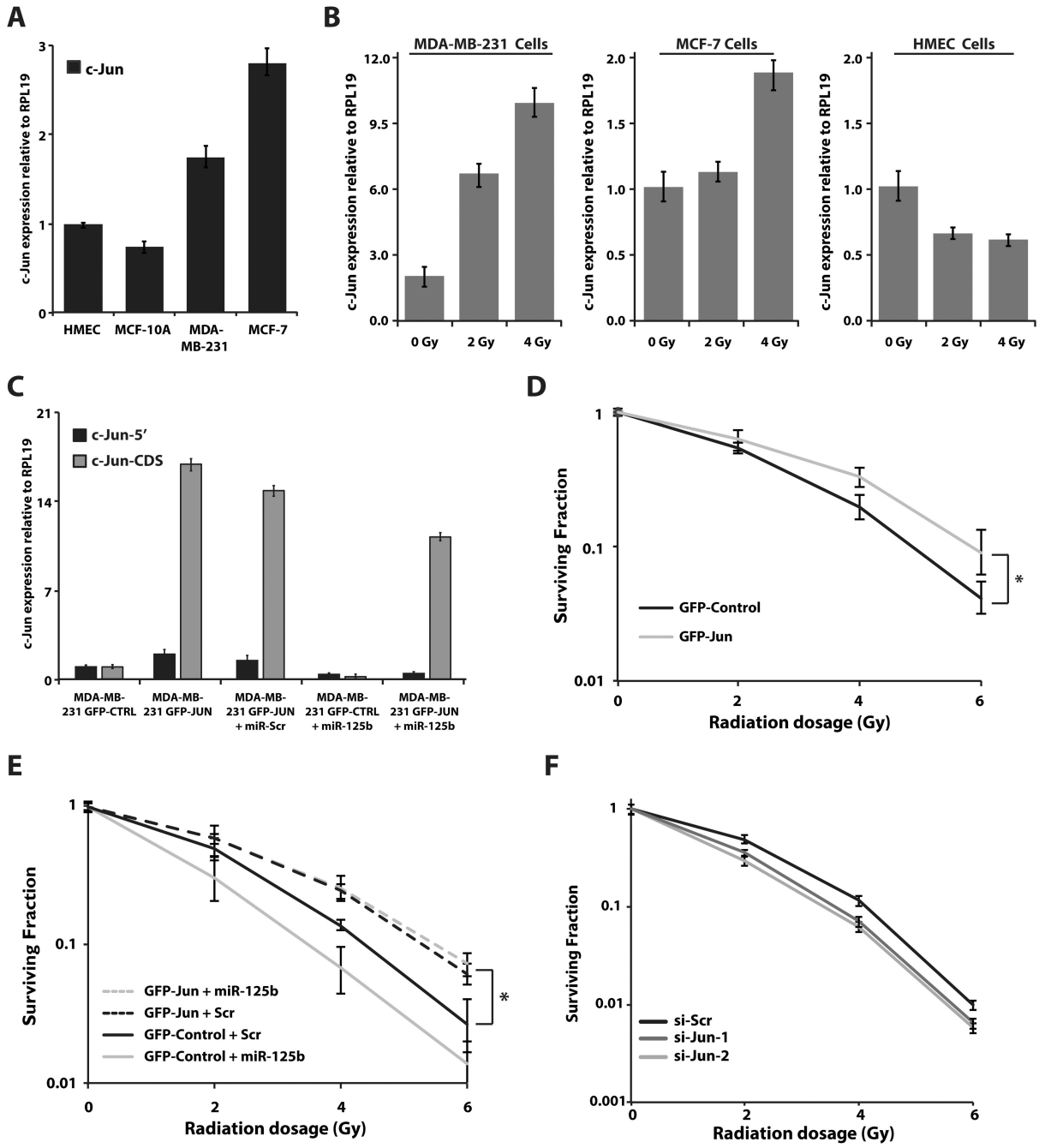


**Figure 5.** ***c-JUN levels increase post-γ-irradiation*** **and promotes radioresistance**

**(A)** qRT-PCR analysis of *JUN* levels in normal HMEC and MCF-10A cells as compared to MDA-MB-231 and MCF-7 breast cancer cells. **(B)** MDA-MB-231 and MCF-7 breast cancer cells, as well as normal HMECs, were irradiated at 0, 2, and 4Gy doses and collected for qRT-PCR analysis 16hrs later. Dose curve indicates endogenous *JUN* levels increased in breast cancer cells but decreased in HMECs post-γ-irradiation. **(C)** qRT-PCR analysis of *JUN* levels in the stable MDA-MB-231 c-JUN-ORF-IRES-GFP line (GFP-Jun). Primers that only recognize the 5′UTR of *JUN* (c-Jun-5′) help differentiate levels of endogenous *JUN* to

those generated by the ORF construct, which are both detected by the coding sequence *JUN* primer set (c-Jun-CDS). **(D)** Analysis of clonogenic assays on MDA-MB-231 c-JUN-ORF-IRES-GFP cells (GFP-Jun) 10 days following γ-irradiation. c-JUN-ORF-IRES-GFP cells (GFP-Jun) harbored higher colony forming potential than stable lines expressing GFP alone (GFP-Control), * *p-value* < 0.01 as determined by 2-way ANOVA. **(E)** Rescue experiments indicating miR-125b could sensitize GFP-Control cells to γ-irradiation, but not c-JUN-ORF-IRES-GFP cells (GFP-Jun). * *p-value* < 0.01 as determined by 2-way ANOVA. **(F)** Clonogenic experiments indicating 2 independent siRNAs to *JUN* can mildly sensitize MCF-7 cells to γ-irradiation, as compared to a scrambled siRNA control (si-Scr).

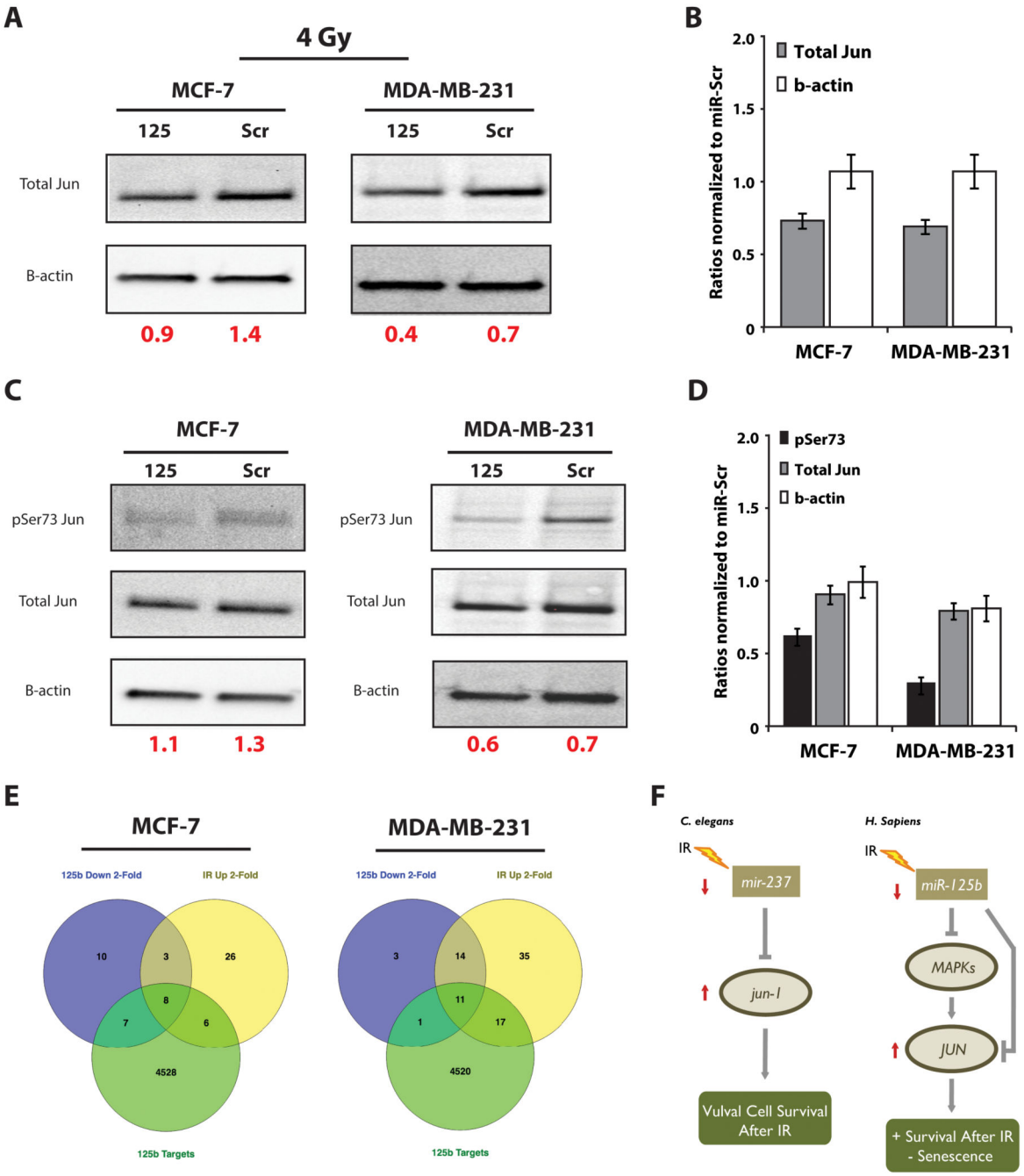


**Figure 6. miR-125b regulates c-JUN activity by influencing the MAPK pathway**

**(A)** Western blot analysis of total c-JUN expression in 4Gy-treated MCF-7 and MDA-MB-231 cells pre-transfected with 30nM miR-125b or miR-Scr control mimic. Values in red indicate the ratio of c-Jun to β-actin within each condition. **(B)** Quantification of (A); ratios of c-Jun and β-actin expression in miR-125b vs. miR-Scr transfected cells. **(C)** Western blot analysis of p-Ser73 and total c-JUN, and β-actin expression in MCF-7 and MDA-MB-231 cells transfected with 30nM miR-125b or miR-Scr control mimic. Values in red indicate the ratio of total c-Jun to β-actin within each condition. **(D)** Quantification of (C); ratios of p-

Ser73, total c-Jun, and β-actin expression in miR-125b vs. miR-Scr transfected cells. **(E)** Venn diagrams depicting results of qPCR array experiments on MCF-7 and MDA-MB-231 cells 72hrs after miR-125b transfection, or after 4Gy treatment. Genes that changed 2-fold or more are reported and are overlapped with all putative miR-125b targets as determined by TargetScan. **(F)** A model for *cel-mir-237*/hsa-miR-125b regulation of cell survival after γ-irradiation. In *C. elegans*, vulval cells actively downregulate *cel-miR-237* (green arrow) to promote *jun-1* expression, which mediates vulval cell survival. In breast cancer cells miR-125b operates in a similar manner, but may also act through the MAPK pathway to promote senescence.

## Table 1
### C elegans miRNA-deletion mutant strains tested for IR-sensitivity

| Human Homolog | Mutant Strain | miRNAs | IR-Effect | *p-value* |
|---|---|---|---|---|
| *miR-27* | *mir-42/43(gk177)* | miR-42/43 | - | 0.000703 |
| *miR-19* | *mir-254(n4470)* | miR-254 | - | 0.000816 |
| ***miR-125*** | ***mir-237(tm2238)*** | **miR-237** | + | ***0.001182*** |
| *miR-27/134* | *mir-42/43/44(nDf49)* | miR-42/43/44 | - | 0.001574 |
| *miR-99/100* | *mir-51(n4473)* | miR-51 | - | 0.001617 |
| *miR-1* | *mir-1(gk276)* | miR-1 | - | 0.002664 |
| *miR-29* | *mir-83(n4638)* | miR-83 | - | 0.003840 |
| *miR-31* | *mir-269(n4641)* | miR-269 | - | 0.007581 |
| *miR-31* | *mir-72(gk166)* | miR-72 | O | 0.151346 |
| *miR-320* | *mir-79(n4126)* | miR-79 | O | 0.195538 |
| *miR-31* | *mir-73/74(nDf47)* | miR-73/74 | O | 0.849273 |
| *miR-193/365* | *mir-240/786(n4541)* | miR-240/786 | ±/O/- | N/A (varied) |

12 miRNA-deletion strains covering 15 miRNAs were tested for IR-induced vulval defects. **+**, indicates a radio-protective effect in the respective mutant strain (i.e. more nematodes with WT vulva); **-**, indicates a radio-sensitization effect (i.e., more nematodes with Pvl and Vul phenotypes). **O**, indicates no observable difference. *p-values* were determined by paired t-test analysis from at least 3 independent experiments.